

Effect of the oxidation conditions on the maghemites produced by laser pyrolysis[†]

S. Veintemillas-Verdaguer,* M. P. Morales and C. J. Serna

Instituto de Ciencia de Materiales de Madrid, C.S.I.C., Cantoblanco 28049, Madrid, Spain

Pure γ -Fe₂O₃ particles were continuously prepared by a continuous wave CO₂ laser-induced pyrolysis of iron pentacarbonyl vapour in an oxidizing atmosphere. Two different oxidation procedures were investigated: (1) air–argon mixtures were employed to fill the apparatus; (2) air–ethylene mixtures were employed as carrier gas. The powders were identified by X-ray diffraction. The grain size was measured using transmission electron microscopy and the degree of order was estimated by IR spectroscopy. The products obtained have grain sizes in the range 4 to 17 nm and different degrees of structural order depending on the synthesis conditions. The productivities attained are typically 0.05 gh⁻¹. Finally, the magnetic properties of the maghemite powders are discussed. It seems that, for very small magnetic particles, the actual differences in the sizes of the particles are less important than differences in crystallinity with regard to the magnetic properties of the samples. Copyright © 2001 John Wiley & Sons, Ltd.

Keywords: maghemite nanoparticles; γ -Fe₂O₃; laser pyrolysis; magnetic measurements

maghemite nanoparticles smaller than 10 nm are mainly used as catalysts and in the production of magnetic fluids suitable for, among other things, biomedical applications.³ Maghemite nanoparticles ranging continuously between 3 and 8 nm can be produced by co-precipitation of iron salts in the presence of additives under controlled conditions.⁴ However, maghemite nanoparticles can also be produced in a continuous process by spray pyrolysis.⁵ Furthermore, a narrower size distribution of these nanoparticles can be currently obtained by laser-induced pyrolysis, as has recently been shown.^{6–9}

Most of the pyrolysis-based processes employed to obtain maghemite nanoparticles started from an Fe³⁺ salt. However, it has been shown that in these procedures the Fe³⁺ is partially reduced to a mixture of Fe²⁺ and Fe³⁺ with the formation of magnetite that finally is oxidized to maghemite. Without the initial reduction step haematite is formed instead of maghemite.¹⁰ In this work the starting point is an iron compound with oxidation degree zero; we expected, as in the previously mentioned processes, that the oxidation procedure would be one of the key parameters of the process. In this paper we present the effect of the experimental oxidation procedure on the maghemite particles produced by laser pyrolysis of iron pentacarbonyl vapour. Special attention will be paid to the particle size, crystalline domain, the structural order and the magnetic properties of the samples.

INTRODUCTION

Small magnetic particles have attracted considerable attention owing to their technological and scientific importance.^{1,2} For example, in particular,

EXPERIMENTAL

Reagent grade Fe(CO)₅, obtained from Aldrich Chemical Inc., was used as the iron precursor owing to its high vapour pressure and easy decomposition. It was stored in the dark at 7 °C under nitrogen, and was employed without purification. Ethylene N35 (99.95%), argon N45 (total impurities below

* Correspondence to: S. Veintemillas-Verdaguer, Instituto de Ciencia de Materiales de Madrid, C.S.I.C., Cantoblanco 28049, Madrid, Spain.

† Based on work presented at the 1st Workshop of COST 523: Nanomaterials, held 20–22 October 1999, at Frascati, Italy
Contract/grant sponsor: CICYT; Contract/grant number: PB95-0002.

Table 1 Experimental parameters used to produce maghemite under hard oxidation conditions.

Sample no.	FE90	FE89	FE88	FE59	FE44
Carrier gas (SCCM)					
Ethylene	5	4	3	2	1
Air	1	2	3	4	5
Consumption (g h^{-1})	0.290	0.159	0.180	0.210	0.240
Production (g h^{-1})	0.104	0.058	0.067	0.076	0.044
Fe_2O_3 yield (%)	88	90	92	91	45
$a(\text{\AA})$	8.36 ± 0.01	8.36 ± 0.03	8.36 ± 0.01	8.36 ± 0.03	—
Scherrer crystallite size (nm)	2.3	3	2.7	2.7	—

11 ppm) and air were provided by Air Liquide España S.A.

The method of synthesis involves heating a flowing mixture of gases with a continuous-wave carbon dioxide laser, which initiates and sustains a chemical reaction. Above a certain pressure and laser power, a critical concentration of product nuclei is formed in the reaction zone. This leads to homogeneous nucleation of particles that are carried to a filter by an inert gas. The experimental setting employed was described in detail previously.⁹ Owing to the non-absorption of the laser wavelength ($10.60 \pm 0.05 \mu\text{m}$) by iron pentacarbonyl, ethylene was used as an absorbent as well as to carry the carbonyl vapour to the reaction zone. The ethylene does not decompose at the energy density employed (652 W cm^{-2}) and simply becomes hot under the laser radiation heating the gas mixture. Under these conditions, iron pentacarbonyl is decomposed into iron and carbon monoxide. In order to obtain iron oxide, a flow of air was introduced into the system. Two different methods were used to introduce the air flow into the system.

- (a) A mixture of air and ethylene was introduced together with the iron pentacarbonyl vapour; the oxidation takes place mainly under the

laser radiation. This process will be termed 'hard oxidation' or briefly 'hard'.

- (b) Air was introduced into the reaction chamber mixed with the argon flux, which is employed to avoid deposition of powder on the laser entrance window.^{6–9} Under this procedure, oxidation takes place mainly after the laser. In the following, this process will be termed 'soft oxidation' or briefly 'soft'.

Tables 1 and 2 list the experimental conditions for both processes. Constant parameters were: laser power, 82 W; argon axial flux, 15 sccm; argon windows flux, 220 sccm; pressure, 400 mbar; reactive weight, 2 g; reactive temperature, 20 °C; average duration of the experiment, 5 h.

No emission of light as observed in the reaction zone in any of the experiments except for sample FE90; the white light emitted indicates a much higher temperature in this case.

The particle size and shape of the samples were determined with a 200 keV Jeol JEM-2000FX transmission electron microscope. The powder was ultrasonically dispersed in toluene and this suspension was deposited onto a carbon-coated copper grid for electron microscopy examination. Identification of the iron oxide phase present in the

Table 2 Experimental parameters used to produce maghemite under soft oxidation conditions; ethylene carrier gas flux 6 sccm.

Sample identification	FE49	FE50	FE45	FE56
Air window flux (sccm)	15	21	27	75
Consumption (g h^{-1})	0.172	0.159	0.219	0.102
Production (g h^{-1})	0.064	0.059	0.083	0.041
Fe_2O_3 yield (%)	91	92	93	98
$a(\text{\AA})$	8.362 ± 0.003	8.351 ± 0.005	8.357 ± 0.001	8.36 ± 0.01
Scherrer crystallite size (nm)	9.0	5.3	3.7	2.8

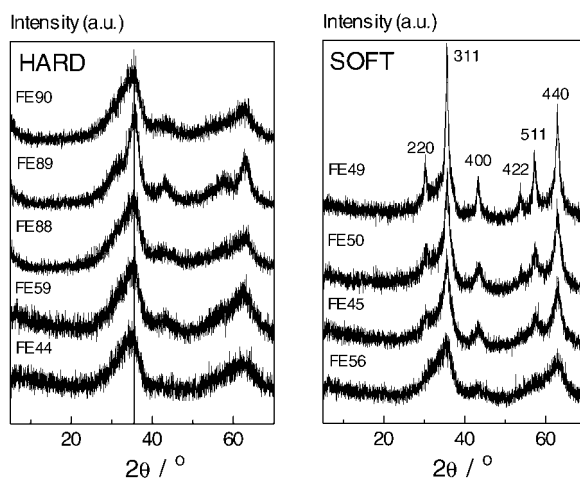


Figure 1 X-ray diffraction patterns of maghemite samples obtained under hard and soft oxidation conditions.

samples was carried out in a Philips PW1710 diffractometer with Cu K α radiation. The X-ray diffraction patterns were recorded between 5 and 70° 2 θ at 0.5° min⁻¹. Lattice parameters and crystallite size determination were obtained from the X-ray diffractograms following standard procedures.¹¹ In some cases the experimental broad and asymmetric peak (311) + (220) of poorly crystallized maghemite samples was deconvoluted into the two components using the peak-fitting utility of the PHYLLIPS-APD computer program. The IR spectra of the samples diluted in KBr were recorded between 850 and 250 cm⁻¹ in a Nicolet 20SXC FT-IR. In this region of the IR spectrum, absorption bands associated with O–Fe modes take place. Magnetic characterization of the samples was carried out in a SQUID magnetometer. Hysteresis loops were recorded at room temperature and at 5 K after applying a saturating field of 5 T. Magnetic parameters, such as saturation magnetization M_s and coercivity H_c , were obtained from the loops for each sample.

RESULTS AND DISCUSSION

X-ray diffraction

The X-ray diffraction patterns of the powders obtained under hard and soft oxidation conditions are shown in Fig. 1. The peaks can be assigned to an iron oxide spinel, similar to maghemite or magne-

tite, for all the samples, and no extra peaks were observed.

Samples prepared under hard oxidation conditions show very broad diffraction peaks, indicating a poorer crystallinity (Fig. 1). It should be noted that the X-ray pattern corresponding to sample FE89 shows narrower peaks than the rest. This is the most crystalline sample within this series, probably due to the Fe/O₂ molar ratio used in the preparation, which was 0.71, close to the stoichiometric value for Fe₂O₃ of 1.33. On the contrary, similar and broad diffraction patterns were obtained for the rest of the samples prepared either with excess of iron, such as sample FE90 (Fe/O₂ = 2.59), or with deficit of iron, such as sample FE44 (Fe/O₂ = 0.43).

In order to identify the iron oxide phase, the cell parameters were calculated from the positions of the peaks (Table 1). A good correlation with the maghemite cell parameter $a = 8.35$ Å was only obtained for samples FE90, FE89, FE88 and FE59. However, for sample FE44, the peak positions are displaced (Fig. 1), probably due to the existence of a mixture of maghemite and another iron oxide. For sample FE44, a low concentration of the sensitizer gas ethylene is used and a lower reaction temperature should be attained, which is also responsible for the decrease in the yield. The Debye–Scherrer crystallite size was estimated in samples FE59, FE88, FE89 and FE90 from the peak width of the (311) reflection. In all cases the crystallite size estimated was around 3 nm (Table 1).

It can be concluded that, under hard oxidation conditions, relatively poorly crystalline particles of about 3 nm of crystalline domains of γ -Fe₂O₃ were

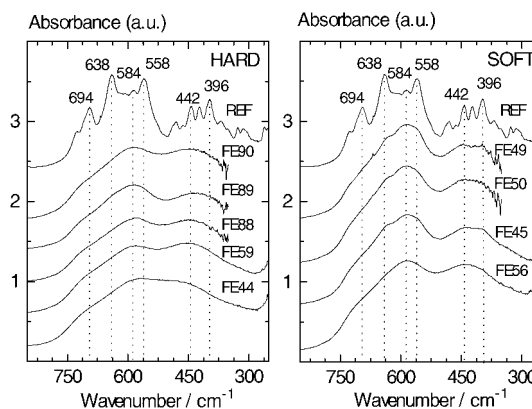


Figure 2 IR spectra of maghemite samples prepared under hard and soft oxidation conditions.

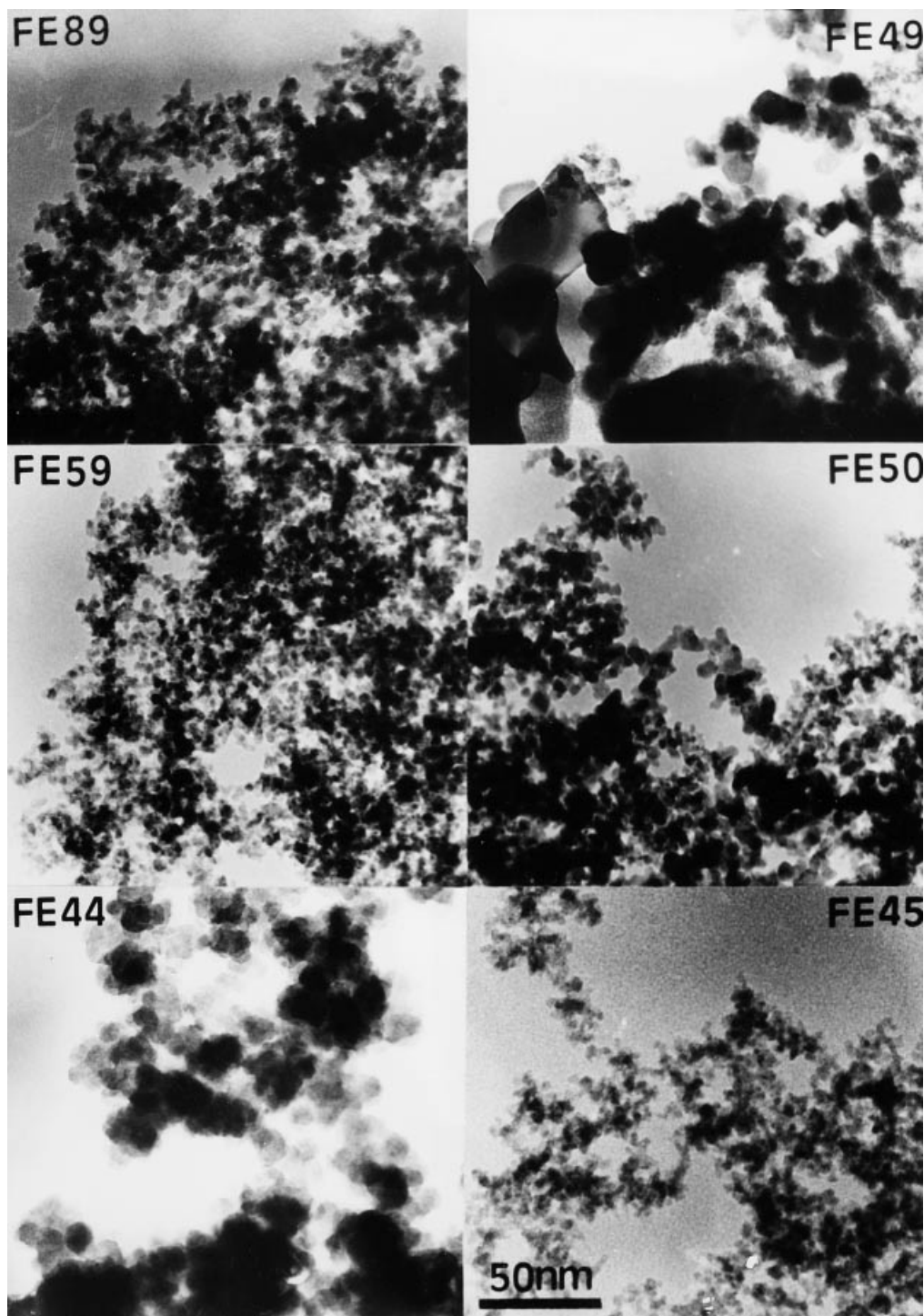


Figure 3 TEM images of maghemite samples prepared under hard oxidation conditions (left) and soft oxidation conditions (right).

Table 3 Magnetic parameters obtained at room temperature and 5 K for the γ -Fe₂O₃ nanoparticles obtained under hard and soft oxidation conditions.

Sample no.	Magnetic properties			
	300 K		5 K	
	M_s (emu g ⁻¹)	H_c (Oe)	M_s (emu g ⁻¹)	H_c (Oe)
<i>Hard oxidation</i>				
FE89	22	0	28	1200
FE59	6	0	10	1800
<i>Soft oxidation</i>				
FE50	21	0	25	800
FE45	21	0	25.5	750

obtained. On the other hand, samples obtained under soft oxidation conditions are much better crystallized (Fig. 1), as can be inferred from the width of the X-ray peaks. The samples are pure maghemite according to the a parameter, which is similar to the reported value and equal to 8.35 Å (Table 2). The Debye–Scherrer crystallite size decreases from 9 nm in sample FE49, obtained under low oxygen excess, to 3 nm in sample FE56, obtained under higher oxygen excess. Therefore, under soft oxidation conditions, particles of γ -Fe₂O₃ with crystalline domains between 3 and 9 nm can be obtained by varying the amount of air introduced to the system.

IR spectroscopy

IR spectra of the maghemite powders in the region corresponding to Fe–O vibrations are depicted in Fig. 2. In the same figure a maghemite sample (REF) composed of spherical particles of 120 nm diameter, in which the octahedral cation vacancies are full ordered,¹² is shown for comparison. The spectra of the samples obtained under hard oxidation conditions, presented in Fig. 2, show the presence of two broad bands at approximately 584 and 442 cm⁻¹ for all the samples except for FE44. Note the absence of fine structure in the bands in comparison with the REF sample, which indicates not only a small particle size but also vacancy disorder.

Samples prepared under soft oxidation conditions showed IR spectra with at least four peaks, at 638, 584, 442 and 396 cm⁻¹, which are less distinct for sample FE56.

Small differences in the relative intensity I of the bands at 584 and 442 cm⁻¹ have been detected and

related to the degree of structural order. In this sense, it has been considered that some order remains in the samples when $I(584)$ is greater than $I(442)$; if the contrary happens the sample is considered fully disordered (e.g. sample FE59). Following this criterion, we conclude that maghemite powders obtained under hard oxidation (Fig. 2) are more disordered than those obtained under soft oxidation conditions (Fig. 2). The degree of order is FE59 < FE88 \approx FE90 < FE89 in the first case and FE56 < FE45 \approx FE50 < FE49 in the second case. It can be seen that IR spectroscopy can distinguish between samples FE59 and FE88, which present very similar XRD patterns, whereas the degree of order parallels the crystallite size in samples prepared by soft oxidation.

TEM analysis

Figure 3 shows the TEM micrographs of selected maghemite samples. About 100 maghemite particles were counted from each picture in order to evaluate the TEM average size. The samples obtained under hard oxidation conditions, FE59 and FE89, consist of spherical particles of approximately 4 nm average size, whereas FE44 has 17 nm average size. From the accordance of the TEM size with the crystallite size obtained by X-ray (Table 1) we conclude that FE59 and FE89 are monocrystalline. The broad X-ray diffraction peaks of sample FE44 suggest that its crystallite size must be very small, in contradiction to its TEM size. Therefore, we conclude that FE44 is polycrystalline.

Different results were found for samples obtained under soft oxidation conditions. Average TEM sizes of 4 nm, 8 nm and 10 nm were measured for samples FE45, FE50 and FE49 respectively, in

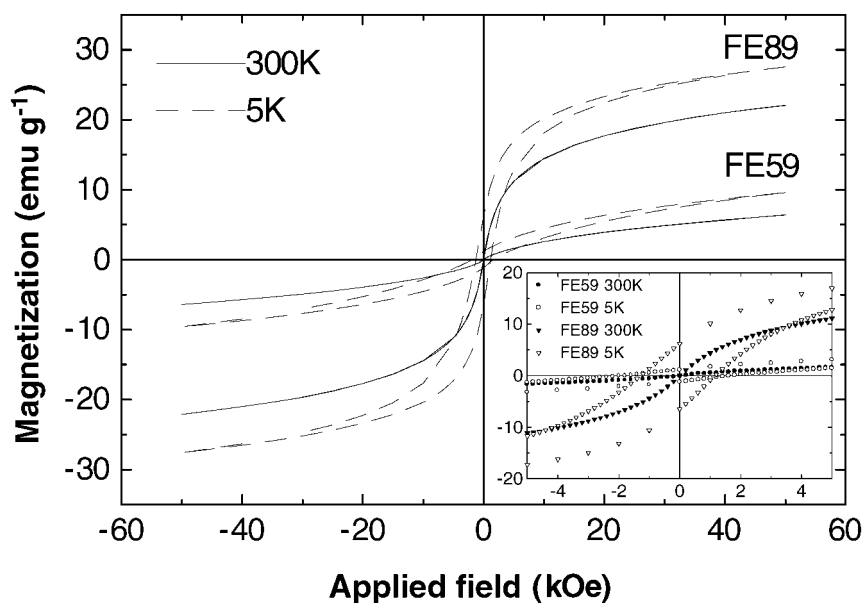


Figure 4 Hysteresis loops at room temperature and 5 K for samples FE59 and FE89 obtained under hard oxidation conditions.

close accordance with the crystallite sizes calculated by X-ray diffraction (Table 2). Consequently, we conclude that the particles forming the above-mentioned samples are monocrystalline.

Magnetic properties

For all the samples, superparamagnetic behaviour at room temperature is expected owing to the small particle size (<10 nm). Magnetic parameters

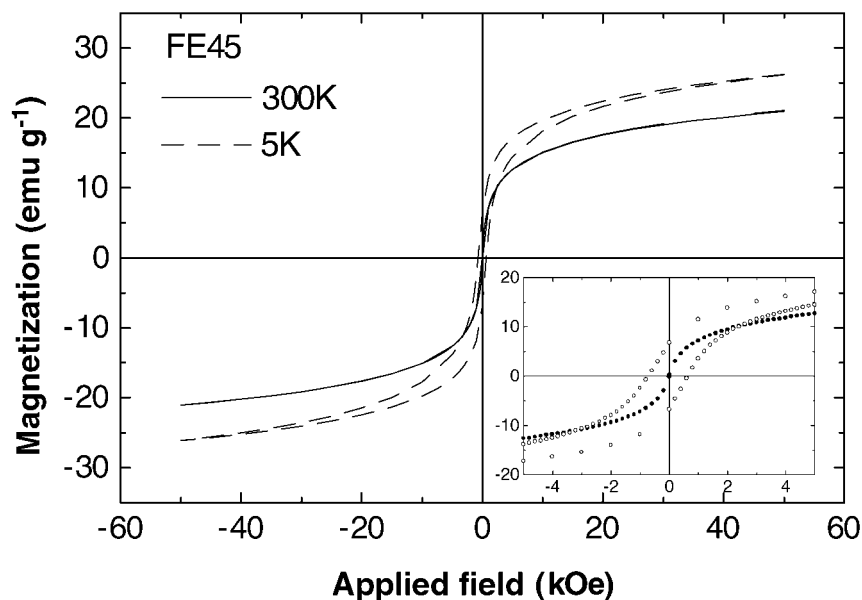


Figure 5 Hysteresis loops at room temperature and at 5 K for sample FE45 obtained under soft oxidation conditions.

obtained for two samples of similar particle sizes and different crystallinities obtained under hard oxidation (FE59, FE89) and two samples of different particle sizes and similar crystallinities obtained under soft oxidation conditions (FE45, FE50) are included in Table 3.

Samples FE59 and FE89, formed by extremely small particles (<3 nm) obtained by hard oxidation, show large crystallinity differences (Fig. 1), which justifies the different values of saturation magnetization obtained at room temperature and 5 K (Table 3). Small particle size is correlated with high surface area, which gives rise to spin canting of the magnetic moments at the particle surface and, therefore, to a reduction of the saturation magnetization from the value reported for γ -Fe₂O₃ bulk. Additionally, internal spin disorder is expected to be present in particles with low crystallinity, giving rise to an extra reduction of the saturation magnetization, as is shown for sample FE59. In agreement with that, very high coercivity values were obtained for both samples, the highest value being obtained for the poorer crystallized sample, FE59 (Table 3). The hysteresis cycles obtained for these samples at room temperature and at 5 K are depicted in Fig. 4.

Samples FE45 and FE50, obtained by soft oxidation and formed by particles of 4 nm and 8 nm respectively and having similar crystallinities, show small differences in saturation magnetization and coercive field, not only at room temperature but also at 5 K (Table 3). The hysteresis cycle obtained for sample FE45, similar to that of FE50, is presented in Figure 5.

From the above results it is clear that (in the range of very small magnetic particles) the crystallinity of magnetic nanoparticles plays a role that has often been undervalued in favour of the particle-size effect. Under hard oxidation conditions, maghemite samples with different magnetic properties due to differences in the particle crystallinity can be obtained, whereas soft oxidation produces maghemite samples with similar magnetic properties.

Formation mechanism

From the previous observations we can propose two different mechanisms for hard and soft oxidation. In the former we suggest that the process is controlled by the ethylene proportion: the first step of the process is the decomposition of iron pentacarbonyl to relatively big iron particles that are subsequently oxidized. In experiment FE44 the decomposition

was incomplete due to the low temperature attained and the high proportion of oxygen; this leads to the fast oxidation of iron particles without crystallization. As the ethylene proportion increases, so also does the temperature and the crystallinity of the product, with the subsequent decomposition of the initial particles leading finally to nanocrystalline maghemite.

Under soft oxidation conditions, the evolution of sizes and polydispersities of the samples with the amount of oxygen present in the atmosphere suggests that an oxidation plus agglomeration process follows the initial quantitative decomposition of the carbonyl. In sample FE45 the oxidation is faster and there is no time for agglomeration. In the experiments FE50 and FE49 (Fig. 3) the oxygen content in the system decreases, the oxidation is slower and more time is available for the agglomeration. Consequently, sample FE49 has the largest particle size and is the most polydisperse and crystalline of the samples synthesized.

CONCLUSIONS

Maghemite nanoparticles of approximately 4 nm of diameter with a high degree of monodispersity can be obtained by laser pyrolysis of a mixture of Fe(CO)₅-C₂H₄-air (hard oxidation). Different degrees of crystallinity and different values of saturation magnetization and coercive fields as a function of the ethylene proportion can be obtained. Well-crystallized maghemite nanoparticles with different sizes ranging from 4 to 8 nm and similar magnetic properties can be obtained by laser pyrolysis of a mixture of Fe(CO)₅-C₂H₄ in an argon-air atmosphere as a function of the proportion of air.

Acknowledgements This research was supported by the CICYT under project PB95-0002.

REFERENCES

1. Ziolo RF, Giannelis EP, Weinstein BA, O'Horo MP, Ganguly BN, Mehrotra V, Russell MW, Huffman DR. *Science* 1992; **257**: 219–223.
2. Awschalom DD, Di Vincenzo DP. *Phys. Today* 1995; **4**: 43–48.
3. Martin CR, Mitchell DT. *Anal. Chem. News Features* 1998; 322A–327A.

4. Bee A, Massart R, Neveu S. *J. Magn. Magn. Mater.* 1995; **149**: 6–9.
5. Gonzalez-Carreño T, Morales MP, Gracia M, Serna CJ. *Mater. Lett.* 1993; **18**: 151–155.
6. Cannon WR, Danforth SC, Flint JH, Haggerty JS, Marra RA. *J. Am. Ceram. Soc.* 1982; **65**: 324–329.
7. Canon WR, Danforth SC, Haggerty JS, Marra RA. *J. Am. Ceram. Soc.* 1982; **65**: 330–335.
8. Alexandrescu R, Morjan I, Cruntenau A, Cojocaru S, Petcu S, Teodorescu V, Huisken F, Kohn B, Ehbrecht M. *Mater. Chem. Phys.* 1998; **55**: 115–121.
9. Veintemillas-Verdaguer S, Morales MP, Serna CJ. *Mater. Lett.* 1998; **35**: 227–231.
10. Pecharroman C, Gonzalez-Carreño T, Iglesias JE. *Phys. Chem. Miner.* 1995; **22**: 21–29.
11. Klug HP, Alexander LE. *X-Ray Diffraction Procedures*. John Wiley and Sons: New York; 1954, Chapter 9.
12. Morales MP, Pecharroman C, Gonzalez-Carreño T, Serna CJ. *J. Solid State Chem.* 1994; **108**: 158–163.